
SVD-Free Low-Rank Adaptive Gradient Optimization for Large Language Models

Ionut-Vlad Modoranu* Mher Safaryan Erik Schultheis Dan Alistarh

¹Institute of Science and Technology Austria (ISTA)

Abstract

Low-rank optimization has emerged as a promising direction in training large language models (LLMs) to reduce the memory usage of adaptive optimizers by constraining learning to a lower-dimensional space. Prior work typically projects gradients of linear layers using approaches based on Singular Value Decomposition (SVD). However, applying SVD-based procedures individually to each layer in large models is computationally expensive and incurs additional memory costs due to storing the projection matrices. In this work, we propose a computationally efficient and conceptually simple two-step procedure to approximate SVD-based gradient projections into lower-dimensional spaces. First, we construct a complete orthogonal basis using predefined orthogonal matrices of the Discrete Cosine Transform (DCT). Second, we adaptively select basis columns based on their alignment with the gradient of each layer. Each projection matrix in our method is obtained via a single matrix multiplication followed by a lightweight sorting step to identify the most relevant basis vectors. Due to the predefined nature of the orthogonal bases, they are computed once at the start of training. During training, we store only the indices of the selected columns, avoiding the need to store full projection matrices for each layer. Our numerical experiments on both pre-training and fine-tuning tasks demonstrate the effectiveness of our dual strategy in approximating optimal low-rank projections, matching the performance of costly SVD-based methods while achieving faster runtime and reduced memory usage.

1 Introduction

The Adam optimizer [Kingma and Ba, 2014] and its regularized version AdamW [Loshchilov and Hutter, 2019] have become the standard approach for optimizing deep neural networks in various settings. With the recent increase in scale of LLMs up to billions and trillions of parameters, training with AdamW becomes more and more challenging, as its internal state requires two momentum buffers that scale with the model size. This practical problem paved the way for a line of research that focuses on reducing the memory usage of optimizer states in the context of adaptive gradient optimization. These approaches range from quantizing the states to 8 bits [Dettmers et al., 2021] to the recent GaLore optimizer [Zhao et al., 2024] inspired from the LoRA techniques [Hu et al., 2021, Lialin et al., 2023], that compresses the gradient matrix using low-rank decomposition based on SVD. Several improvements to GaLore have been proposed to enhance its performance, such as LDAdam [Robert et al., 2025], FRUGAL [Zmushko et al., 2024], FIRA [Chen et al., 2024], BAdam [Luo et al., 2024], Q-GaLore [Zhang et al., 2024b]. The key aspect of GaLore and its later improvements is the low-rank decomposition based on matrix factorization, such as SVD or QR decomposition. These techniques are known to be computationally intensive as they have to be invoked for each linear layer, either at each step (for, e.g., LDAdam) or once at a few steps (for, e.g., GaLore). To mitigate the high cost of SVD, we ask: *can we find an alternative projection to serve as*

*Correspondence to ionut-vlad.modoranu@ista.ac.at

an accurate replacement for the orthogonal matrices in SVD, that is much cheaper to compute, and portable across memory-efficient optimizers?

Contributions. In this work, we address our research question by proposing a cheaper alternative to the orthogonal matrices computed via SVD. Concretely, we propose using the orthogonal matrices from the general class of Discrete Fourier Transforms, such as the Discrete Cosine Transform (DCT), which has been successfully used in image compression for the JPEG algorithm. To the best of our knowledge, we are the first to use it in the context of low-rank adaptive gradient optimization. We summarize our contributions as follows:

- We show the DCT matrix is an accurate replacement for the orthogonal matrices computed via SVD. We reduce the running time and improve the memory usage as we store only one DCT matrix for the entire network, computed once at the beginning of the training. Instead of storing one projection matrix for each layer, we just have to store r (rank) integers, representing the indices of most significant columns for that particular layer.
- We propose a theory-based approach to compute the most significant columns of the DCT matrix to obtain a dynamic projection matrix tailored to each layer.
- In order to show that DCT matrices accurately approximate the orthogonal matrices of SVD, we add the DCT transformation into existing low-rank optimizers and show they recover training loss, memory usage and/or running time.
- We propose a standalone optimizer that uses the DCT projection and optionally adds quantized error feedback for the projection error, rotates the momentum buffers such that new low-rank gradients are correctly incorporated and allows changing the low-rank subspace every step.

2 Related Work

We review the prior work in the literature focused on reducing the running time and memory usage of optimizers by compressing the gradient, especially by low-rank compression. Most approaches use individual projection matrices tailored to the gradient at each layer by invoking techniques based on quantization or matrix factorization, such as SVD, QR or PCA. One pioneering work in the context of low-rank adaptive optimization is the recent GaLore optimizer [Zhao et al., 2024] which performs SVD once at a few steps to project the gradient to a lower-dimensional space. GaLore was followed by several other optimizers that improve certain aspects of it.

The first improvement aspect is the running time, which forces GaLore to compute SVD once at a few steps in order to be feasible in practice for large models. LDAdam [Robert et al., 2025] compresses the first order momentum in AdamW, replaces SVD with a block power-iteration [Bentbib and Kanber, 2015] and performs a smooth subspace transition by rotating the first and second momentum accordingly to incorporate gradients from the same subspace at each step.

The second improvement aspect is convergence. By default, GaLore discards the projection error, which LDAdam stores and incorporates into the gradient at the next step. In contrast, the recent work FRUGAL [Zmushko et al., 2024] makes the distinction between the low-rank gradient (called state-full) and the projection error (called state-free). The state-full gradient is used in AdamW, while the state-free gradient is fed to an optimizer without state, such as SignSGD. The main idea is to leverage the remaining gradient information in the projection error since it is available at each step instead of discarding or storing it. A concurrent work to FRUGAL is FIRA [Chen et al., 2024], which aims to preserve the low-rank constraint for memory efficiency while achieving full-rank performance by proper scaling of the projection error.

In addition to improvements over GaLore, some prior work focuses on achieving memory usage similar to SGD while preserving the performance of AdamW. Apollo [Zhu et al., 2024] exploits the redundancy in the computed adaptive learning rates of AdamW and shows that element-wise learning rate is not necessary. As a consequence, they focus on computing one adaptive learning rate per channel, which significantly improves the memory usage and throughput by allowing larger batch sizes due to memory savings. They achieve this by projecting the gradient to a lower-dimensional space using a random matrix only to compute the scaling for the gradient, which remains full-rank.

Another approach worth mentioning is Online Subspace Descent [Liang et al., 2024], which replaces SVD projection with Online PCA, which involves computing the projection matrix as a solution of

an optimization function focused on 1) minimizing the projection error and 2) forcing the projection matrix to be orthogonal. The authors indicate that performing one step with Adam to solve this additional optimization problem is enough to obtain a qualitatively good projection matrix P . In contrast, our method does not introduce such overheads during training since the DCT projection is already computed at the beginning of training.

As complementary approaches to low-rank compression, there is some prior work worth mentioning due to their similar goal of reducing the memory usage and running time with a different methods than low-rank. AdamW-8bit [Dettmers et al., 2021] quantizes the states of AdamW optimizer to 8-bits using efficient CUDA kernels, with the effect of reducing the memory usage by a half compared to bfloat16 and without introducing additional computational overheads. In the same spectra of methods we find MicroAdam [Modoranu et al., 2024], where the optimizer states are compressed via sparsity and error feedback. Adam-mini [Zhang et al., 2024a] reduces optimizer states memory by assigning a single learning rate to each parameter block carefully partitioning the parameter matrix into blocks.

Despite all aforementioned approaches being similar in using SVD-based projections, they differ in a few aspects. The most important one in our view is how they handle the projection error and how often they update the low-dimensional subspace, which we clarify in Table 1.

Our approach uses DCT projection coupled with a dynamic column selection to determine a projection matrix tailored to the gradient for a particular layer, can use any update frequency and can be integrated into any optimizer, regardless of the way it handles the projection error.

Table 1: Properties of prior low-rank adaptive optimizers. The update frequency* 200 is the default in GaLore that made the approach computationally feasible.

Low-rank Projection	Type	Frequency*	Error
GaLore [Zhao et al., 2024]	SVD	200	discard
Frugal [Zmushko et al., 2024]	SVD, Random, RandPerm	200	feed to SignSGD
Fira [Chen et al., 2024]	SVD	200	norm-based scaling
Subspace Descent [Liang et al., 2024]	Online PCA	1	discard
LDAdam [Robert et al., 2025]	Block Power Iteration	1	error feedback
DCT-AdamW (this work)	DCT	1	error feedback

3 Method

This section introduces the orthogonal DCT matrix we use to replace SVD, the technique to dynamically choose columns to obtain a projection matrix tailored to the gradient at each layer, as well as the standalone optimizer DCT-AdamW we propose.

3.1 Discrete Cosine Transform

The Discrete Cosine Transform (DCT) is widely used in the signal processing and data compression (e.g., JPEG algorithm for image compression) and consists of n orthogonal basis vectors whose components are cosines [Strang, 1999]. There are minor variations of DCT and in this work we will use DCT-2 and DCT-3 (one is the transpose of the other). We denote the DCT-3 matrix of order n by $Q \in \mathbb{R}^{n \times n}$, defined as $Q_{ij} = \sqrt{2/n} \cdot \cos \frac{i(2j+1)\pi}{2n}$, with $i, j \in [n]$, where the first row has to be divided by $\sqrt{2}$ in order for Q to be orthogonal, i.e. $Q^\top Q = I_n$. We can efficiently compute Q using a vectorized implementation that is fast for large values of n on the GPU as follows. We first create one vector $L = [0, \dots, n-1]^\top$, which is used to create the matrix $\mathcal{I} \in \mathbb{N}^{n \times n}$ by replicating L on the columns of \mathcal{I} :

$$L = \begin{bmatrix} 0 \\ 1 \\ \vdots \\ n-1 \end{bmatrix} \quad \mathcal{I} = \begin{bmatrix} 0 & \cdots & 0 \\ 1 & \cdots & 1 \\ \vdots & \cdots & \vdots \\ n-1 & \cdots & n-1 \end{bmatrix}_{n \times n} \quad Q = \sqrt{\frac{2}{n}} \cos \left(\frac{\mathcal{I} \odot (2\mathcal{I}^\top + 1)}{2n} \pi \right)$$

We restate that we need to divide the first row by $\sqrt{2}$ to make Q orthogonal. The computational efficiency comes from the element-wise product $\mathcal{I} \odot (2\mathcal{I}^\top + 1)$ that actually computes the integer entries $i(2j+1)$. Once we compute Q , we can use it as a replacement for the SVD procedure in conjunction with the dynamic selection of columns, which we explain in detail next.

3.2 Dynamic Selection of Columns

General View. After computing the DCT matrix $Q \in \mathbb{R}^{n \times n}$, we need to compute a projection matrix $Q_r \in \mathbb{R}^{n \times r}$ by selecting r columns from Q to project the gradient $G \in \mathbb{R}^{n \times n}$ to an r -dimensional space $g = GQ_r \in \mathbb{R}^{n \times r}$. First, we compute $S = GQ$ containing the scalar products between rows of G and columns of Q . We rank the columns of S based on their L_1 -norm and then pick the largest r columns, which we use in Q_r . The i^{th} column in matrix S contains the scalar products between rows of G and column i of Q . We view these scalar products as similarities and we want to choose the columns of Q with largest similarity with rows of G . Since the columns of Q are defined as cosines of different frequencies at each component, we state that columns of Q act as a filter for the rows of G . We choose L_1 -norm because we do not want the similarities to be altered, as it would be the case for L_2 -norm. Using this approach, we ensure a dynamic mechanism to choose the most appropriate columns of Q for the current gradient matrix G . Each layer will have its own set of r indices for the columns. The case illustrated so far is for a general square matrix G . In the context of GaLore, where $G \in \mathbb{R}^{n \times m}$, we reduce the smallest dimension of G to r , which means we have to take into consideration two cases, based on the relationship between n and m .

The first case is $n \geq m$, which is known as “right projection” in GaLore, where $Q \in \mathbb{R}^{m \times m}$ is the DCT-3 matrix. We compute $S = GQ$ and the corresponding $Q_r \in \mathbb{R}^{m \times r}$ contains the most significant r columns of S . The second case is $n < m$, which is known as “left projection” and this time we compute $S = Q^\top G$, where we are interested in the rows of Q and columns of G . Here, $Q^\top \in \mathbb{R}^{n \times n}$ is the DCT-2 matrix (the transpose of DCT-3, but we store only the DCT-3 matrix, Q) and in order to choose the columns of Q we have to select r indices of the largest rows in S .

Usually, the smallest dimension of the gradient matrix is the hidden size of the model d_{model} . As a result, the memory overhead of replacing the SVD projection with the DCT matrix and the dynamic selection of columns is storing a single matrix $Q \in \mathbb{R}^{d_{\text{model}} \times d_{\text{model}}}$ for the entire model and r integers for the corresponding columns from Q for each layer.

3.3 DCT-AdamW

We propose DCT-AdamW, a standalone low-rank version of AdamW with DCT projection that has the option to use quantized error feedback (EF) [Seide et al., 2014, Karimireddy et al., 2019, Alistarh et al., 2018] and ensures momentum buffers integrate gradients from the same lower dimensional subspaces as in LDAdamW [Robert et al., 2025]. In contrast to LDAdamW, which has to store two consecutive projection matrices per layer, we only have to store two sets of r indices due to simplicity of our DCT approach coupled with the dynamic column selection technique. Prior work MicroAdam [Modoranu et al., 2024] quantized the error feedback down to 4-bits in the context of compressing the optimizer state using sparsity. In our context, we observed that the lowest resolution we can quantize EF to is 8-bits. We state our optimizer in Algorithm 1.

Algorithm 1 DCT-AdamW (right projection)

```

1: Input:  $\beta_1, \beta_2, \epsilon, T, T_u, r$ 
2:  $m_0, v_0 \leftarrow 0_{n \times r}, 0_{n \times r}$ 
3:  $\Xi_1 \leftarrow 0_{n \times m}$   $\diamond$  error feedback (EF) buffer
4:  $Q \in \mathbb{R}^{m \times m}$   $\diamond$  DCT matrix
5:  $\mathcal{I}_{\text{crt}}, \mathcal{I}_{\text{prev}} \leftarrow 0_r, 0_r$   $\diamond$  column indices
6: for  $t = \{1, 2, \dots, T\}$  do
7:    $G_t \leftarrow \nabla_\theta f(\theta_t) + \Xi_t$ 
8:    $R \leftarrow \text{UPDATESUBSPACE}(G_t)$ 
9:    $g_t \leftarrow G_t \cdot Q_{\text{crt}}$   $\diamond$  projected gradient
10:   $\Xi_t \leftarrow G_t - g_t \cdot Q_{\text{crt}}^\top$   $\diamond$  update EF
11:   $m_t \leftarrow \beta_1 \cdot m_{t-1} \cdot R + (1 - \beta_1)g_t$ 
12:   $v_t \leftarrow \beta_2 |v_{t-1} \cdot R| + (1 - \beta_2)g_t^2$ 
13:   $\theta_{t+1} \leftarrow \theta_t - \eta_t \frac{\hat{m}_t}{\epsilon + \sqrt{v_t}} Q_{\text{crt}}^\top$ 
14: end for

```

Algorithm 2 Update Subspace procedure

```

1: procedure UPDATESUBSPACE( $G$ )
2:    $R \leftarrow I_{r \times r}$   $\diamond$  switching matrix between
3:   consecutive low-rank spaces
4:   if  $t > 1$  then
5:      $\mathcal{I}_{\text{prev}} \leftarrow \mathcal{I}_{\text{crt}}$ 
6:   end if
7:   if  $(t = 1) \vee (t \bmod T_u = 0)$  then
8:     re-rank the columns and
9:      $\mathcal{I}_{\text{crt}} \leftarrow \text{RANKCOLS}(GQ, r)$ 
10:    update the switching matrix
11:     $R \leftarrow Q_{\text{prev}}^\top \cdot Q_{\text{crt}}$ 
12:   end if
13:   return  $R$ 
14: end procedure

```

The sets $\mathcal{I}_{\text{prev/crt}}$ hold the indices of the r columns for the previous/current projections and $Q_{\text{prev/crt}}$ contain the columns from Q specified by the these two sets. T_u represents the subspace update interval (set to 200 for GaLore and to 1 for LDAdam). The procedure RANKCOLS ranks the columns

of $S = G_t \cdot Q$ as explained in Section 3.2. In order to make sure the momentum buffers integrate gradients from the same subspaces, we need to rotate m_t and v_t using a rotation matrix R that first projects the momentum to the full-dimensional space using the previous projector and then projects it back to the current lower-dimensional subspace. We can perform this rotation directly in the r -dimensional space by multiplying the two projection matrices, resulting in $R \in \mathbb{R}^{r \times r}$. Rotating v_t might introduce negative values and we apply the absolute value function to force the non-negativity of v_t . The low-rank gradient g_t is computed by multiplying the full-rank gradient G_t with Q_{crt} and the full-rank update is obtained multiplying u_t by Q_{crt}^\top .

4 Memory Savings and Running Time

In this section we provide details about running time and memory savings after replacing the expensive SVD with DCT, coupled with the dynamic column selection approach.

4.1 Memory Savings

For simplicity, we compute the memory usage for a generic model with L layers, each of size $n \times n$ for a fixed rank r and provide concrete values for the Llama-2 7B model, for which $n = 4096$.

SVD. To perform the low-rank decomposition for a gradient matrix $G \in \mathbb{R}^{n \times n}$, we use the SVD decomposition $G = U\Sigma V^\top$ and use the first r columns of U as a projection matrix $P = U_{:,r}$. Storing one projection matrix P for each of the L layers in the neural network leads to storing additional Lnr elements only for the projection matrices.

DCT. To perform low-rank decomposition using DCT, we have to store the DCT matrix $Q \in \mathbb{R}^{n \times n}$ that will be the same for all layers and r additional indices at each layer, which will be used to extract the corresponding columns. Finally, the total number of elements to be stored is $n^2 + Lr$. Usually, n is the hidden dimension of the model d_{model} , which the memory usage directly depends on.

Practical Memory Usages. We compute the memory usage for a Llama-2 7B model to understand the practical implications of using a constant orthogonal matrix compared to SVD-based projections. Table 2 shows the memory usage of our approach is not sensitive to rank, since we only store r integers instead of individual projection matrices with r columns. Instead, the memory usage of SVD depends on both hidden dimension of the model $n = d_{\text{model}}$ and the rank, since r columns have to be stored. This translates to memory savings for our approach for LLMs. In DDP settings, we store one projection matrix for each GPU. However, when the model size becomes too large, GPUs can store different columns of the matrix to prevent materializing the full projection matrix on each GPU.

Table 2: Practical memory usage for low-rank projection matrices for Llama-2 7B.

	SVD			DCT		
	$r = 32$	$r = 256$	$r = 512$	$r = 32$	$r = 256$	$r = 512$
bfloat16	56 MiB	448 MiB	896 MiB	32.03 MiB	32.22 MiB	32.44 MiB
float32	112 MiB	896 MiB	1792 MiB	64.03 MiB	64.22 MiB	64.44 MiB

4.2 Running Time

Once the projection matrices P are computed and stored, the computational complexity of the up/down-projection operations is the same as for SVD, as each involves a matrix multiplication between the projection matrix (or its transpose) and the full/low-rank gradient. However, since our projection matrices are based on the Discrete Cosine Transform (DCT), we can leverage fast Fourier transform (FFT) algorithms to reduce the complexity of the up/down-projection operations from $\mathcal{O}(n^2)$ to $\mathcal{O}(n \log n)$. It is important to note that our method for computing the projection matrices is fundamentally different from existing approaches. In this work, we primarily focus on comparing the runtime of our method with that of SVD-based approaches.

For a generic matrix $G \in \mathbb{R}^{n \times n}$, the computational complexity of SVD is $\mathcal{O}(n^3)$. This complexity has to be incurred for each layer once at T_u steps because this procedure is too expensive to be run with higher frequency. On the other hand, our approach computes $S = GQ$, ranks the columns in S by computing L_1 -norm per column and selects the top- r columns to form the projection matrix

P to be used for up/down-projection. At steps where we recompute the projection, we can avoid an additional matrix multiplication between P and the full rank gradient matrix G by returning the largest r columns of S as the low-rank gradient. Overall, our approach has a lower computational overhead compared to the SVD approach, which can also be seen in the running time row of results in experimental section.

5 Theoretical Guarantees

In this section, we provide a theoretical justification for our two-step procedure to approximate SVD-based gradient projections. First, we rigorously show that adaptively selecting columns of an orthogonal matrix based on their alignment with the gradient matrix is an optimal strategy for minimizing the reconstruction error. This approach leads to a contractive compression scheme, which is commonly exploited in the analysis of compressed adaptive optimization algorithms. Next, to justify the specific use of the DCT matrix, we demonstrate that it naturally serves as a linear approximation of the left or right eigenbases of the gradient matrices.

5.1 Optimality of norm-based ranking procedure

Let $G \in \mathbb{R}^{n \times m}$ be the gradient matrix and $Q \in \mathbb{R}^{n \times n}$ is orthogonal, namely $QQ^\top = I_n$ (without loss of generality, we consider left multiplication). For a given rank $r \leq n$, let Q_r be a $n \times r$ sub-matrix of Q composed of r columns. We are interested in the reconstruction error between G and $Q_r Q_r^\top G$, where Q_r^\top performs projection and Q_r performs back-projection. While we may choose any matrix norm to measure the reconstruction error, the standard Frobenius norm makes the derivation cleaner. Specifically, using the definition of the Frobenius norm $\|G\|_F^2 = \text{tr}(G^\top G)$, linearity of trace and $Q_r^\top Q_r = I_r$ due to orthogonality of Q , we decompose the reconstruction error:

$$\begin{aligned} \|G - Q_r Q_r^\top G\|_F^2 &= \text{tr}(G^\top (I - Q_r Q_r^\top)^\top (I - Q_r Q_r^\top) G) = \text{tr}(G^\top (I - Q_r Q_r^\top) G) \\ &= \text{tr}(G^\top G - G^\top Q_r Q_r^\top G) = \text{tr}(G^\top G) - \text{tr}(G^\top Q_r Q_r^\top G) \\ &= \|G\|_F^2 - \|Q_r^\top G\|_F^2 = \|G\|_F^2 - \sum_{i=1}^r \|q_i^\top G\|_2^2, \end{aligned}$$

where q_i 's are the columns of Q_r . From this identity, we conclude that to minimize the reconstruction error, the optimal strategy is to maximize the alignments $\|q_i^\top G\|_2^2$ for all selected columns q_i . Furthermore, since $\|q_1^\top G\|_2^2 + \|q_2^\top G\|_2^2 + \dots + \|q_n^\top G\|_2^2 = \|Q^\top G\|_F^2 = \text{tr}(G^\top Q Q^\top G) = \text{tr}(G^\top G) = \|G\|_F^2$, following the optimal strategy of selecting r columns from Q , we have $\|G - Q_r Q_r^\top G\|_F^2 = \|G\|_F^2 - \sum_{i=1}^r \|q_i^\top G\|_2^2 \leq \|G\|_F^2 - \frac{r}{n} \sum_{i=1}^n \|q_i^\top G\|_2^2 = (1 - \frac{r}{n}) \|G\|_F^2$. Thus, the proposed norm-based selection strategy for any orthogonal matrix Q induces a low-rank compression scheme that is contractive with a factor $1 - r/n$. Contractiveness of the compression scheme is the key property in the convergence analysis of compressed optimization [Stich et al., 2018, Richtárik et al., 2021, Li et al., 2022, Modoranu et al., 2024, Robert et al., 2025].

We can extend the above argument for any p -norm over vectorized matrices, for which the Frobenius norm is the special case of $p = 2$. Then, we have

$$\begin{aligned} \|G - Q_r Q_r^\top G\|_p &= \left\| \sum_{i=1}^n q_i q_i^\top G - \sum_{i=1}^r q_i q_i^\top G \right\|_p = \left\| \sum_{i=r+1}^n q_i q_i^\top G \right\|_p \stackrel{(a)}{\leq} \sum_{i=r+1}^n \|q_i q_i^\top G\|_p \\ &\stackrel{(b)}{=} \sum_{i=r+1}^n \|q_i\|_p \|q_i^\top G\|_p \stackrel{(c)}{\leq} \max(1, n^{\frac{1}{p} - \frac{1}{2}}) \sum_{i=r+1}^n \|q_i^\top G\|_p, \end{aligned}$$

where (a) follows from the triangle inequality of the p -norm, (b) follows from the definition of p -norms for matrices, namely $\|uv^\top\|_p = (\sum_{i,j} u_i^p v_j^p)^{1/p} = (\sum_i u_i^p \sum_j v_j^p)^{1/p} = \|u\|_p \|v\|_p$ for two column-vectors u and v of the same size, (c) follows from the relationship between ℓ_p norms and that $\|q_i\|_2 = 1$, i.e., $\|v\|_p \leq n^{\frac{1}{p} - \frac{1}{2}} \|v\|_2$ if $p \leq 2$ and $\|v\|_p \leq \|v\|_2$ if $p \geq 2$.

5.2 DCT as linear approximation of the gradient eigenbasis

Given a real-valued gradient matrix $G \in \mathbb{R}^{n \times m}$ and its SVD decomposition $G = U\Sigma V^\top$, our goal is to find fast approximation of (without loss of generality) its left eigenvectors stacked in $U \in \mathbb{R}^{n \times n}$. As $GG^\top = U\Sigma^2 U^\top$, it is equivalent to approximate the eigenvectors of symmetric matrix GG^\top .

Our argument starts from a linear algebra decomposition result, originally motivated by the optical information processing literature to factorize linear transformations that can be implemented optically

[Müller-Quade et al., 1998, Schmid et al., 2000]. The result states that any square matrix M of shape $n \times n$ over the complex numbers \mathbb{C} can be decomposed into a product of diagonal and circulant matrices, i.e., $M = D_1 C_2 D_3 \dots D_{2k-3} C_{2k-2} D_{2k-1}$, where D 's are diagonal matrices and C 's are circulant matrices. Circulant matrices are a special class of Toeplitz matrices in which each row is a cyclic right shift of the previous one as shown below:

$$C = \begin{bmatrix} c_0 & c_1 & c_2 & \cdots & c_{n-1} \\ c_{n-1} & c_0 & c_1 & \cdots & c_{n-2} \\ \vdots & \vdots & \cdots & \vdots & \vdots \\ c_1 & c_2 & \cdots & c_{n-1} & c_0 \end{bmatrix}, \quad F = \frac{1}{\sqrt{n}} [w^{ij}]_{i,j=0}^{n-1}, \text{ where } w = e^{\frac{2\pi i}{n}}. \quad (1)$$

The number of factors $2k - 1$ in this decomposition has been shown to be up to $2n - 1$ for almost all matrices (in the sense of Lebesgue measure), and it is further conjectured that a decomposition with up to n factors is sufficient [Huhtanen and Perämäki, 2015]. Since circulant matrices can be diagonalized using the discrete Fourier transform (DFT) matrix F (see (1)), i.e., $C = F^* D F^2$ [Golub and Van Loan, 2013], we can decompose the matrix $F^* M F$ with $M = G G^\top$ and arrive at the following decomposition for $G G^\top$:

$$G G^\top = (F D_1 F^*) D_2 (F D_3 F^*) D_4 \cdots D_{2k-2} (F D_{2k-1} F^*). \quad (2)$$

Notice the analogy between this matrix decomposition and the Taylor expansion for functions. Since the space of matrices is finite-dimensional, the signal-matrix can be recovered using finitely many “variable” D 's, in contrast to the infinite series required for function expansions. Keeping this analogy in mind, just as loss functions are linearly approximated at each iteration in first-order optimization algorithms, we consider a “linear” approximation of the decomposition (2) by including only a single variable D , i.e., $G G^\top \approx F D_1 F^*$.

This directly implies that we approximate the eigenvectors U by the DFT matrix F . However, since the matrix $G G^\top$ is real and symmetric by design, its eigenvalues are real, and the real part $\text{Re}(F)$ also forms an approximate eigenbasis that better aligns with U . Finally, we observe that the real part $\text{Re}(F)$ corresponds to the discrete cosine transform (DCT), up to minor variations.

6 Experiments

We now present our numerical results. Our main goal is to show that DCT projection can recover the performance of SVD-based projection and have lower memory footprint and running time.

For pre-training, we use a Llama model [Touvron et al., 2023] with 800 million parameters and train it on the C4 dataset using 20/100 tokens/parameter, equivalent to 16/80B tokens. We replace the SVD projection in Frugal and Fira with DCT matrix to directly compare the optimizer behavior when the only difference is the projection. We use a learning rate tuned for the full-rank AdamW baseline to avoid the expensive learning rate tuning process for each individual projection. As a result, in certain cases, the DCT projection would require further learning rate tuning. In all settings, our main comparison is against the SVD-like projection and we will also add the full-rank AdamW results for reference. For fine-tuning, we use Llama-2 7B and report the accuracy on GSM-8k dataset [Cobbe et al., 2021] using Frugal and Fira with SVD and DCT projections, as well as on LDAdamW and our DCT-AdamW implementation.

6.1 Pre-training (PT)

We train the Llama-800M model from scratch using 16B and 80B tokens, equivalent to 20 and 100 tokens per parameter, from C4 dataset [Raffel et al., 2020]. The hidden dimension of the model is 2048 and we use rank $r = 256$ for all runs, as well as learning rate $\eta = 7.5e-5$, which was chosen for the full-rank AdamW, proportionally to the inverse square root of the number of parameters and kept fixed for all runs.

PT with FRUGAL. We integrate the DCT matrix into the FRUGAL optimizer and compare against the SVD, RandPerm and Random projections. RandPerm uses a random permutation as a projection matrix, while Random generates a random, semi-orthogonal matrix. In Figure 1a we show the

² F^* is the conjugate transpose of the complex matrix F .

training loss for all these runs. In the zoomed-in plot for the last 5000 training steps we see that SVD projection recovers the performance full-rank AdamW, while the DCT projection is a good approximation of the SVD, which supports our claim. We present our numerical results in Table 3. We would like to emphasize the running time reduced by 1h 48m ($\approx 22.6\%$) compared to the SVD projection, as well as the memory usage reduced by about 2.2GB ($\approx 3.5\%$), while the increase in perplexity is less than one point. In comparison to RandPerm and Random projections, the runtime is on par, while train and validation perplexities are lower by approximately one point in the favor of DCT, illustrating again the benefit of our approach.

PT with FIRA. We integrate DCT into FIRA optimizer and compare against SVD. In Figure 1b we show the training loss, where our focus is on the comparison between SVD and DCT projections. We observe that DCT consistently yields lower training loss compared to the SVD projection, which is also visible in the numerical results in Table 3, translated to lower perplexities in the favor of DCT. Moreover, the memory usage is smaller by 2GB ($\approx 3\%$) and the running time is lower by 1h 54m ($\approx 23.8\%$).

Table 3: Pre-training Results for AdamW, FRUGAL and FIRA with different projections using 20 tokens/parameter. DCT is a good approximation to SVD with lower runtime and memory. AdamW is the full-rank optimizer and is added for reference.

	FRUGAL					FIRA	
	AdamW	SVD	DCT	RandPerm	Random	SVD	DCT
Train PPL	15.55	15.35	15.63	16.52	17.02	19.37	18.88
Val. PPL	14.05	14.02	14.23	15.18	15.61	17.67	17.30
Mem. (GiB)	73.49	65.70	63.50	65.44	63.72	68.44	66.48
Time	7h 54m	9h 45m	7h 57m	7h 56m	7h 56m	9h 53m	7h 59m

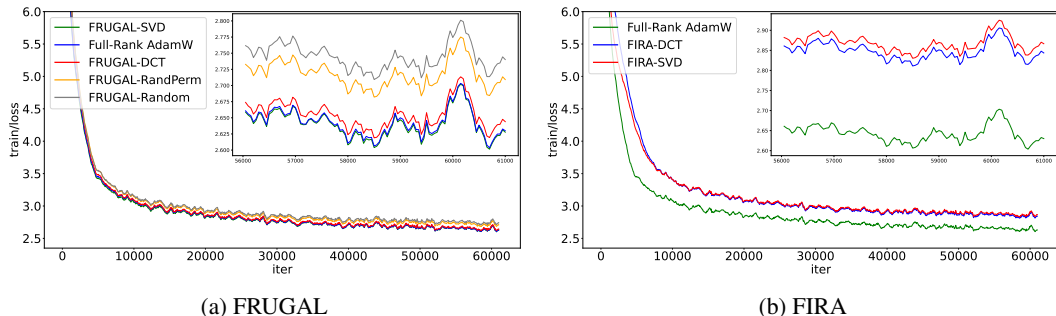


Figure 1: Pre-training Llama-800M using FRUGAL and FIRA on 16B tokens from C4.

PT with LDAdamW. We train Llama-800M on 80B tokens (100 tokens/parameter) from C4 using LDAdam and DCT-AdamW described in Algorithm 1. In particular for our approach, we use EF quantized to 8-bits and some further optimizations from the zero-redundancy optimizer [Rajbhandari et al., 2020], where one layer is updated on a single GPU and then it is broadcasted to the other GPUs. This way, we obtain lower memory usage by replacing redundant operations in the optimizer with communication, since the GPUs receiving the updated layer parameters do not allocate any state, at the cost of slightly increased running time due to more communication. In Figure 2 we present the training loss curves for full-rank AdamW (for reference), LDAdamW and DCT-AdamW and we are interested in directly comparing the last two. We observe that DCT-AdamW has lower training loss than LDAdamW, which also translates to lower perplexities in Table 4. Due to relatively high rank, the memory usage of LDAdamW is close to the memory usage of AdamW because it stores two projection matrices to be able to rotate the momentum buffers. In contrast, DCT-AdamW stores only two sets of r indices instead of storing the actual projection matrices, which drastically reduces the memory usage, coupled with the zero-redundancy trick. In terms of running time, DCT-AdamW is faster than LDAdamW by 10h 7m ($\approx 25.75\%$) and slower than AdamW by 1h 55m ($\approx 5\%$).

Table 4: Pre-training results on Llama-800M for AdamW, LDAdamW and DCT-AdamW with 100 tokens/parameter. AdamW is the full-rank optimizer and is added for reference.

	AdamW	LDAdamW	DCT-AdamW
Train PPL	12.88	15.10	14.95
Val. PPL	11.73	13.91	13.69
Mem. (GiB)	73.72	72.10	57.82
Time	1d 13h 22m	2d 1h 24m	1d 15h 17m

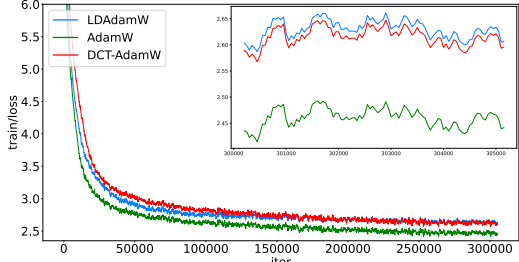


Figure 2: Pre-training Llama-800M with DCT-AdamW and LDAdam on 80B tokens from C4.

6.2 Fine-tuning (FT)

We finetune Llama-2 7B on GSM-8k dataset using SVD and DCT projections for FRUGAL and FIRA optimizers, as well as LD-AdamW and DCT-AdamW. We show our results for ranks $r \in \{32, 512\}$ in Table 5.

FT with FRUGAL. Both projections yield similar training loss for both rank values, which is an indication that DCT is indeed a good approximation for SVD. Despite having different training loss, the SVD projection achieves the same accuracy for both ranks. It is surprising that DCT yields better accuracy for lower rank compared to higher rank. In terms of memory usage, as expected for this large model, the DCT projection saves 8GB of memory ($\approx 23.4\%$) for $r = 32$, while for $r = 512$ the reduction in memory is only 6.3GB ($\approx 18.2\%$). The running time is reduced by roughly 35m ($\approx 75\%$) for both ranks.

Table 5: Fine-tuning results for Llama-2 7B on the GSM-8K dataset.

	FRUGAL				FIRA				LD/DCT-AdamW			
	rank 32		rank 512		rank 32		rank 512		rank 32		rank 512	
	SVD	DCT	SVD	DCT	SVD	DCT	SVD	DCT	LD	DCT	LD	DCT
Train Loss	0.046	0.059	0.051	0.071	0.123	0.209	0.094	0.192	0.261	0.176	0.101	0.208
Acc. (%)	33.81	35.93	33.81	34.26	32.15	32.45	34.27	35.25	31.38	30.09	35.61	35.17
Mem. (GB)	39.61	31.59	40.68	34.41	32.72	31.29	35.41	34.11	32.08	31.17	35.58	34.35
Time	1h 22m	46m	1h 19m	47m	1h 8m	1h	1h 9m	1h	55m	48m	1h 8m	48m

FT with FIRA. The DCT projection yields larger training loss compared to SVD. DCT recovers the accuracy, outperforms the SVD for large rank, and on average reduces the memory usage by ≈ 1.35 GB and the running by ≈ 10 m.

FT with LDAdamW & DCT-AdamW. In this setting we compare the DCT projection with the block power-iteration used in LDAdamW as an approximation to SVD, both without EF. The training loss achieved is smaller for DCT on $r = 32$ and larger for $r = 512$ compared to LDAdamW. LDAdamW achieves more than 1% accuracy for $r = 32$ and comparable accuracy for $r = 512$. Regarding memory, DCT-AdamW uses ≈ 1 GB less memory, while achieving a speedup of about 20m for $r = 512$. We would like to emphasize that EF does not help DCT-AdamW in comparison to LDAdamW for $r = 32$, the accuracy of DCT-AdamW with EF being 29.11% vs 32.53% for LDAdam with EF for $r = 32$, while for $r = 512$ the accuracy can be recovered, scoring 35.33% compared to 35.86% for LDAdamW with EF.

7 Limitations

While our approach shares the underlying principle of low-rank gradient approximation with optimizers like GaLore, FRUGAL, FIRA, and LDAdamW, it is distinctly designed with the computational challenges and scalability demands of large language models (LLMs) in mind. As such, our evaluation and optimization strategy are tailored to this setting, and we leave exploration in domains like computer vision to future work.

References

D. Alistarh, T. Hoefler, M. Johansson, S. Khirirat, N. Konstantinov, and C. Renggli. The convergence of sparsified gradient methods, 2018. URL <https://arxiv.org/abs/1809.10505>.

A. Bentbib and A. Kanber. Block Power Method for SVD Decomposition. *Analele Stiintifice ale Universitatii Ovidius Constanta, Seria Matematica*, 23:45–58, 06 2015. doi: 10.1515/auom-2015-0024.

X. Chen, K. Feng, C. Li, X. Lai, X. Yue, Y. Yuan, and G. Wang. Fira: Can we achieve full-rank training of llms under low-rank constraint?, 2024. URL <https://arxiv.org/abs/2410.01623>.

K. Cobbe, V. Kosaraju, M. Bavarian, M. Chen, H. Jun, L. Kaiser, M. Plappert, J. Tworek, J. Hilton, R. Nakano, C. Hesse, and J. Schulman. Training verifiers to solve math word problems, 2021. URL <https://arxiv.org/abs/2110.14168>.

T. Dettmers, M. Lewis, S. Shleifer, and L. Zettlemoyer. 8-bit optimizers via block-wise quantization. *arXiv preprint arXiv:2110.02861*, 2021.

G. H. Golub and C. F. Van Loan. *Matrix Computations - 4th Edition*. Johns Hopkins University Press, Philadelphia, PA, 2013. doi: 10.1137/1.9781421407944. URL <https://epubs.siam.org/doi/abs/10.1137/1.9781421407944>.

E. J. Hu, Y. Shen, P. Wallis, Z. Allen-Zhu, Y. Li, S. Wang, L. Wang, and W. Chen. Lora: Low-rank adaptation of large language models, 2021. URL <https://arxiv.org/abs/2106.09685>.

M. Huhtanen and A. Perämäki. Factoring matrices into the product of circulant and diagonal matrices. *Journal of Fourier Analysis and Applications*, 2015.

S. P. Karimireddy, Q. Rebjock, S. U. Stich, and M. Jaggi. Error feedback fixes signsgd and other gradient compression schemes, 2019. URL <https://arxiv.org/abs/1901.09847>.

D. P. Kingma and J. Ba. Adam: A method for stochastic optimization, 2014.

X. Li, B. Karimi, and P. Li. On distributed adaptive optimization with gradient compression. *arXiv preprint arXiv:2205.05632*, 2022.

V. Lialin, N. Shivagunde, S. Muckatira, and A. Rumshisky. Relora: High-rank training through low-rank updates, 2023. URL <https://arxiv.org/abs/2307.05695>.

K. Liang, B. Liu, L. Chen, and qiang liu. Memory-efficient LLM training with online subspace descent. In *The Thirty-eighth Annual Conference on Neural Information Processing Systems*, 2024. URL <https://openreview.net/forum?id=P8rTCT6g45>.

I. Loshchilov and F. Hutter. Decoupled weight decay regularization. In *Proceedings of the Seventh International Conference on Learning Representations*, 2019.

Q. Luo, H. Yu, and X. Li. BAdam: A memory efficient full parameter training method for large language models. *arXiv preprint arXiv:2404.02827*, 2024.

I.-V. Modoranu, M. Safaryan, G. Malinovsky, E. Kurtic, T. Robert, P. Richtarik, and D. Alistarh. Microadam: Accurate adaptive optimization with low space overhead and provable convergence, 2024. URL <https://arxiv.org/abs/2405.15593>.

J. Müller-Quade, H. Aagedal, T. Beth, and M. Schmid. Algorithmic design of diffractive optical systems for information processing. *Physica D: Nonlinear Phenomena*, 120(1):196–205, 1998. ISSN 0167-2789. doi: [https://doi.org/10.1016/S0167-2789\(98\)00055-4](https://doi.org/10.1016/S0167-2789(98)00055-4). URL <https://www.sciencedirect.com/science/article/pii/S0167278998000554>. Proceedings of the Fourth Workshop on Physics and Consumption.

C. Raffel, N. Shazeer, A. Roberts, K. Lee, S. Narang, M. Matena, Y. Zhou, W. Li, and P. J. Liu. Exploring the limits of transfer learning with a unified text-to-text transformer. *Journal of machine learning research*, 21(140):1–67, 2020.

S. Rajbhandari, J. Rasley, O. Ruwase, and Y. He. Zero: Memory optimizations toward training trillion parameter models. In *SC20: International Conference for High Performance Computing, Networking, Storage and Analysis*, pages 1–16. IEEE, 2020.

P. Richtárik, I. Sokolov, and I. Fatkhullin. EF21: A New, Simpler, Theoretically Better, and Practically Faster Error Feedback. *arXiv preprint arXiv:2106.05203*, 2021.

T. Robert, M. Safaryan, I.-V. Modoranu, and D. Alistarh. Ldadam: Adaptive optimization from low-dimensional gradient statistics, 2025. URL <https://arxiv.org/abs/2410.16103>.

M. Schmid, R. Steinwandt, J. Müller-Quade, M. Rötteler, and T. Beth. Decomposing a matrix into circulant and diagonal factors. *Linear Algebra and its Applications*, 306(1):131–143, 2000. ISSN 0024-3795. doi: [https://doi.org/10.1016/S0024-3795\(99\)00250-5](https://doi.org/10.1016/S0024-3795(99)00250-5). URL <https://www.sciencedirect.com/science/article/pii/S0024379599002505>.

F. Seide, H. Fu, J. Droppo, G. Li, and D. Yu. 1-bit stochastic gradient descent and its application to data-parallel distributed training of speech DNNs. In *Fifteenth Annual Conference of the International Speech Communication Association*, 2014.

S. U. Stich, J.-B. Cordonnier, and M. Jaggi. Sparsified SGD with memory. *arXiv preprint arXiv:1809.07599*, 2018.

G. Strang. The discrete cosine transform. *SIAM review*, 41(1):135–147, 1999.

H. Touvron, T. Lavril, G. Izacard, X. Martinet, M.-A. Lachaux, T. Lacroix, B. Rozière, N. Goyal, E. Hambro, F. Azhar, A. Rodriguez, A. Joulin, E. Grave, and G. Lample. Llama: Open and efficient foundation language models, 2023.

Y. Zhang, C. Chen, Z. Li, T. Ding, C. Wu, D. P. Kingma, Y. Ye, Z.-Q. Luo, and R. Sun. Adam-mini: Use Fewer Learning Rates To Gain More. *arXiv preprint arXiv:2406.16793*, 2024a.

Z. Zhang, A. Jaiswal, L. Yin, S. Liu, J. Zhao, Y. Tian, and Z. Wang. Q-GaLore: Quantized galore with int4 projection and layer-adaptive low-rank gradients. *arXiv preprint arXiv:2407.08296*, 2024b.

J. Zhao, Z. Zhang, B. Chen, Z. Wang, A. Anandkumar, and Y. Tian. Galore: Memory-efficient llm training by gradient low-rank projection. *arXiv preprint arXiv:2403.03507*, 2024.

H. Zhu, Z. Zhang, W. Cong, X. Liu, S. Park, V. Chandra, B. Long, D. Z. Pan, Z. Wang, and J. Lee. Apollo: Sgd-like memory, adamw-level performance. *arXiv preprint arXiv:2412.05270*, 2024.

P. Zmushko, A. Beznosikov, M. Takáč, and S. Horváth. Frugal: Memory-efficient optimization by reducing state overhead for scalable training, 2024. URL <https://arxiv.org/abs/2411.07837>.

Contents

1	Introduction	1
2	Related Work	2
3	Method	3
3.1	Discrete Cosine Transform	3
3.2	Dynamic Selection of Columns	4
3.3	DCT-AdamW	4
4	Memory Savings and Running Time	5
4.1	Memory Savings	5
4.2	Running Time	5
5	Theoretical Guarantees	6
5.1	Optimality of norm-based ranking procedure	6
5.2	DCT as linear approximation of the gradient eigenbasis	6
6	Experiments	7
6.1	Pre-training (PT)	7
6.2	Fine-tuning (FT)	9
7	Limitations	9
A	Hyper-parameters and Reproducibility	13
A.1	Pre-training	13
A.1.1	Model	13
A.1.2	Hyper-Parameters	13
A.2	Fine-tuning	13
A.2.1	Model	13
A.3	Hardware	13
B	Extended Experiments	13
B.1	Pre-training	13
B.2	Fine-tuning	14
B.2.1	Llama-2-7b on Viggo & SQL	15
B.2.2	Llama-3-8b on GSM-8k, Viggo & SQL	16
B.2.3	Particularity of Llama-3-8B architecture	17

A Hyper-parameters and Reproducibility

In this section we provide details about the hyper-parameters we used to obtain the results in the main paper, including hardware description, in order to reproduce the results.

A.1 Pre-training

A.1.1 Model

We use the [`llm-baselines`](https://github.com/epfml/llm-baselines)³, a public repository that implements the Llama architecture from scratch and allows creating models with different number of parameters. We use the version with 822M parameters. We would like to emphasize that the number of parameters stated here does not include the embeddings and classification head, which have both size 65.5M (if included, then total model size is 953M parameters). The model has 16 Llama blocks with embedding size 2048 and 16 attention heads.

For our experiments, we train the models from scratch using 20 and 100 tokens per parameter. The linear layers are trained using the optimizers mentioned in the paper, while the embeddings, classification head and layer normalization layers are trained with AdamW.

A.1.2 Hyper-Parameters

Due to the lengthy training time of pretraining, we performed tuning over a limited range of learning rates for all optimizers. We selected learning rates that scale with $\propto 1/\sqrt{d}$, where d represents the model size. Our learning rate grid consisted of $\{7.5e-5, 1e-4, 2.5e-4\}$ for the experiments involving 20 tokens per parameter. For settings with 100 tokens per parameter, we refrained from performing any grid search because the process would be computationally intensive, and consequently, we maintained the learning rate fixed at $7.5e-5$.

A.2 Fine-tuning

A.2.1 Model

We use the [`llm-foundry`](https://github.com/mosaicml/llm-foundry)⁴ repository to finetune Llama-2-7B⁵ and Llama-3 8B⁶ pretrained by Meta and we download the models from HuggingFace.

A.3 Hardware

We use NVidia H100 80GB GPUs for all experiments. For pre-training, we used PyTorch DPP with 8 GPUs and for fine-tuning we used only one GPU per experiment.

B Extended Experiments

B.1 Pre-training

We extend the experimental section in the main paper by adding experiments with Apollo optimizer for pre-training in the setting with 20 tokens per parameter. We would like to emphasize that FRUGAL uses the same learning rate as in the main paper (i.e. $7.5e-5$), while the other optimizers (FIRA, Apollo and GaLore) have slightly larger learning rate obtained via grid search (i.e. $2.5e-4$, compared to $7.5e-5$ in the main paper). In these experiments we use rank $r = 256$.

³<https://github.com/epfml/llm-baselines>

⁴<https://github.com/mosaicml/llm-foundry>

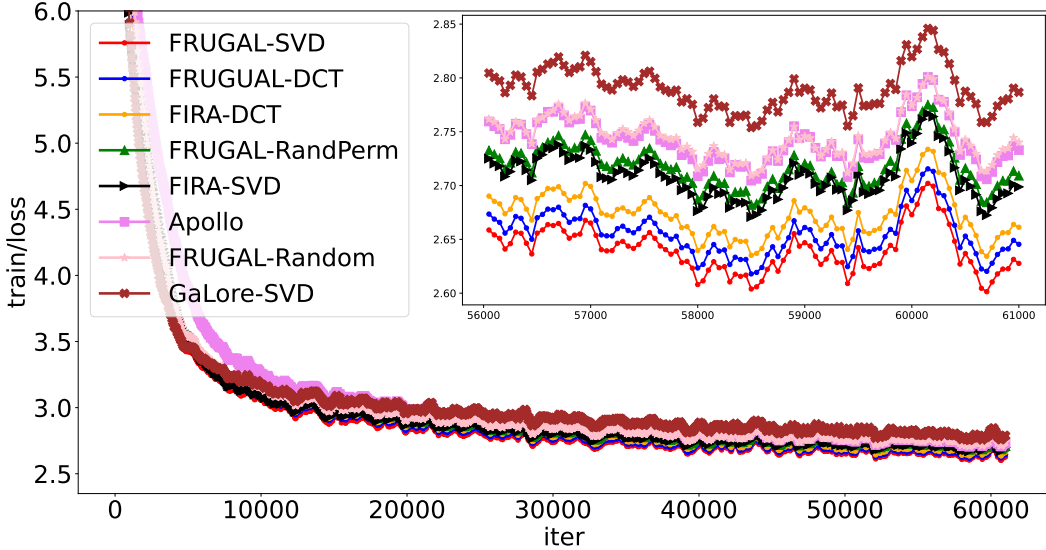
⁵<https://huggingface.co/meta-llama/Llama-2-7b>

⁶<https://huggingface.co/meta-llama/Meta-Llama-3-8B>

Table 6: Extended pre-training experiments for AdamW, FRUGAL and FIRA with different projections using 20 tokens/parameter. DCT is a good approximation to SVD with lower runtime and memory. LR stands for Learning Rate.

Optimizer	Projection	LR	Train PPL	Val. PPL	Mem. (GiB)	Time
FRUGAL	SVD	$7.5e - 5$	15.35	14.02	65.70	9h 45m
	DCT		15.63	14.23	63.50	7h 57m
	RandPerm		16.52	15.18	65.44	7h 56m
	Random		17.02	15.61	63.72	7h 56m
FIRA	SVD	$2.5e - 4$	19.37	17.67	68.44	9h 53m
	DCT		18.88	17.30	66.48	7h 59m
Apollo	Random	$2.5e - 4$	17.00	15.53	67.40	7h 56m
GaLore	SVD	$2.5e - 4$	17.82	16.32	69.90	9h 32m
DCT-AdamW	DCT	$2.5e - 4$	18.22	16.66	68.66	7h 42m

Figure 3: Pre-training Llama-800M with FRUGAL (SVD, DCT, RandPerm, Random), FIRA (SVD, DCT), Apollo (Random) and GaLore (SVD).



B.2 Fine-tuning

We extend the experimental section in the main paper by adding experiments on Llama-2-7b on VIGGO and SQL datasets and on Llama-3-8b on GSM-8k, VIGGO and SQL. We train for 3 epochs on GSM-8k and VIGGO and for one epoch on SQL.

B.2.1 Llama-2-7b on Viggo & SQL

Table 7: Fine-tuning results for Llama-2 7B on the VIGGO dataset. (*) The score a/b for LD means that a didn't have EF and b had EF. (**) The score $a/b/c$ for DCT means that a was run without rotating states and $T_u = 200$, b was run with rotating states and $T_u = 200$ and c was run with rotating states and $T_u = 1$, all without EF. Red values mean we would need an extended learning rate grid because the reported accuracy was obtained at the end of the grid.

Method	Rank	Projection	Acc. (%)	Mem. (GB)	Time
FRUGAL	32	SVD	95.10	39.69	50m
		DCT	95.09	31.49	32m
	512	SVD	89.21	40.67	48m
		DCT	96.08	34.11	33m
FIRA	32	SVD	87.11	32.62	48m
		DCT	91.87	31.38	35m
	512	SVD	92.15	35.16	50m
		DCT	94.96	34.12	33m
GaLore	32	SVD	81.65	32.38	47m
		DCT	41.45	31.38	34m
	512	SVD	94.54	35.18	48m
		DCT	80.39	34.13	32m
LD/DCT-AdamW	32	LD*	67.92 / 87.39	31.89	40m
		DCT**	44.25 / 75.07 / 85.15	31.15	35m
	512	LD*	86.97 / 96.91	35.11	48m
		DCT**	43.13 / 16.67 / 42.85	34.16	32m

Table 8: Fine-tuning results for Llama-2 7B on the SQL dataset

Method	Rank	Projection	Train Loss	Acc. (%)	Mem. (GB)	Time
FRUGAL	32	SVD	0.049	22	39.47	1h 28m
		DCT	0.035	11.8	31.51	1h 6m
	512	SVD	0.060	46.4	40.77	1h 28m
		DCT	0.021	29.9	34.28	1h 3m
FIRA	32	SVD	0.044	81.1	32.39	1h 28m
		DCT	0.062	49.3	31.16	1h 3m
	512	SVD	0.043	57.9	35.29	1h 29m
		DCT	0.026	87.9	34.05	1h 3m
GaLore	32	SVD	0.044	80.7	32.17	1h 26m
		DCT	0.039	81.6	31.16	1h 1m
	512	SVD	0.068	78.5	35.30	1h 26m
		DCT	0.037	86	34.06	1h 1m
LD/DCT-AdamW	32	LD	0.053 / 0.094	42.2 / 66	31.74	1h 8m
		DCT	0.038 / 0.03 / 0.036	77.1 / 79.6 / 56.4	31.05	1h 4m
	512	LD	0.04 / 0.032	53.9 / 32.7	35.1	1h 25m
		DCT	0.032 / 0.035 / 0.046	86.9 / 36.3 / 87.9	34.09	1h 1m

B.2.2 Llama-3-8b on GSM-8k, Viggo & SQL

Table 9: Fine-tuning results for Llama-3 8B on the GSM-8K dataset. (*) means the best performance was obtained on the largest learning rate in the grid (larger learning rate might help). See also Appendix B.2.3.

Method	Rank	Projection	Train Loss	Acc. (%)	Mem. (GB)	Time
FRUGAL	32	SVD	0.066	35.70	52.25	1h 6m
		DCT	0.049	39.04	42.35	51m
	512	SVD	0.077	38.74	54.35	1h 8m
		DCT	0.054	40.18	44.74	50m
FIRA	32	SVD	0.233	59.74	41.69	1h 8m
		DCT	0.237	59.97	41.38	50m
	512	SVD	0.192	59.97	45.91	1h 8m
		DCT*	0.122	52.61	44.53	53m
GaLore	32	SVD	0.299	61.26	41.70	1h 4m
		DCT*	0.334	55.5	41.38	48m
	512	SVD	0.182	60.65	45.87	1h 4m
		DCT*	0.317	56.02	44.51	48m
LD/DCT-AdamW	32	LD	0.262	59.97	40.73	54m
		DCT	0.220 / 0.239 / 0.204	53.6 / 56.10 / 47.46	41.34	49m
	512	LD*	0.115	56.78	45.12	1h 5m
		DCT*	0.240 / 0.282 / 0.126	57.46 / 52.84 / 42.15	44.51	50m

Table 10: Fine-tuning results for Llama-3 8B on the VIGGO dataset. See also Appendix B.2.3.

Method	Rank	Projection	Acc. (%)	Mem. (GB)	Time
FRUGAL	32	SVD	94.67	52.20	45m
		DCT	93.98	42.3	34m
	512	SVD	91.6	54.3	46m
		DCT	93.84	44.42	34m
FIRA	32	SVD	95.94	41.64	45m
		DCT	96.5	41.32	34m
	512	SVD	95.94	45.85	45m
		DCT	95.08	44.45	34m
GaLore	32	SVD	95.23	41.65	45m
		DCT	93.98	41.32	33m
	512	SVD	95.52	45.81	45m
		DCT	94.81	44.41	33m
LD/DCT-AdamW	32	LD	78.99	40.66	40m
		DCT	95.24	41.3	35m
	512	LD	84.87	45.06	48m
		DCT	95.65	44.45	36m

Table 11: Fine-tuning results for Llama-3 8B on the SQL dataset. See also Appendix B.2.3.

Method	Rank	Projection	Train Loss	Acc. (%)	Mem. (GB)	Time
FRUGAL	32	SVD	0.056	77.4	51.23	1h 26m
		DCT	0.071	76.9	42.30	1h 8m
	512	SVD	0.084	73.5	54.32	1h 28m
		DCT	0.073	34.6	44.67	1h 10m
FIRA	32	SVD	0.062	78.4	41.64	1h 26m
		DCT	0.054	79.5	41.32	1h 10m
	512	SVD	0.054	79.2	45.86	1h 27m
		DCT	0.048	79.5	44.5	1h 11m
GaLore	32	SVD	0.066	77.7	41.64	1h 22m
		DCT	0.071	77.2	41.13	1h 5m
	512	SVD	0.063	79.3	45.85	1h 23m
		DCT	0.058	79.5	44.29	1h 6m
LD/DCT-AdamW	32	LD	0.032	79.7	40.47	1h 10m
		DCT	0.074 / 0.041 / 0.063	64.4 / 77.3 / 78.1	41.3	1h 9m
	512	LD	0.073	80.5	45.09	1h 30m
		DCT	0.047 / 0.056 / 0.071	78.8 / 77.1 / 77.9	43.52	1h 8m

B.2.3 Particularity of Llama-3-8B architecture

We would like to mention a significant different in the architecture of Llama-3-8B in comparison with Llama-2-7B that disadvantages the DCT projection.

First of all, the main idea of our work is to store one DCT matrix of shape $n \times n$, where n is the embedding dimension. For Llama-2-7b, we can easily store a single DCT matrix because the smallest dimension of all linear layers is $n = 4096$. However, in the case of Llama-3-8B, the MLP projections for the values (i.e. `v_proj`) have shapes $(1024, 4096)$, where 4096 is the embedding dimension. According to the GaLore rules, these layers should be projected on the left because the smallest dimension is 1024. Performing a left projection would mean we need a DCT matrix of order 1024 such that the dimension of the projected gradient for this layer is $(r, 4096)$. We do not want to store a second DCT matrix of shape $(1024, 1024)$ and as a consequence we decided to perform right projection in this case, since we already have the DCT matrix of shape $(4096, 4096)$ already allocated. As a result, the projected layer will have the shape $(1024, r)$. We would like to emphasize that this design choice affects the results for Llama-3-8B because the MLP layers `v_proj` are embedded to a much lower dimensional space and has the potential of becoming a bottleneck in the network.

The idea we suggest to solving this issue without allocating a new DCT matrix is to use the first 1024 rows and 1024 columns of the DCT matrix of size $(4096, 4096)$ (properly scaled with a factor that is proportional to $\sqrt{4096/1024}$) such that the resulting submatrix is orthogonal and perform the left projection as in the original GaLore.